Electronic Supplementary Information (ESI)

"Epimers *vs.* inverse epimers: the C-1 configuration in alnumycin A1"

Petri Tähtinen,*[a] Terhi Oja,[b] Nadine Dreiack,[a,b] Pekka Mäntsälä,[b] Jarmo Niemi,[b] Mikko Metsä-Ketelä[b] and Karel D. Klika*[a]

Abstract. The determination of whether two stereoisomers constitute a pair of epimers or if they differ in their configuration at all stereogenic centers bar one can be a formidable challenge and represent a more formidable problem than absolute configuration determination *per se*. The latter case is hereby defined as a pair of inverse epimers and is exemplified by alnumycin A1 to introduce the concept.

[a] *Department of Chemistry, University of Turku, Vatselankatu 2, FIN-20014, Turku, Finland. E-mail: klikakd@yahoo.co.uk; petri.tahtinen@utu.fi; Fax: +358 (0)2 333 6700; Tel: +358 (0)2 333 6804*
[b] *Department of Biochemistry and Food Chemistry, University of Turku, Vatselankatu 2, FIN-20014, Turku, Finland.*

Contents:

NMR spectroscopy

NMR spectra were acquired using a Bruker Avance NMR spectrometer equipped with either a 5-mm inverse or a 5-mm normal configuration probe, both with z-gradient capability, at a field strength of 11.75 T operating at 500 and 125 MHz for ^{1}H and ^{13}C nuclei, respectively, at 25 °C with samples contained in $CDCl_3$. The chemical shifts of ^{1}H and ^{13}C nuclei are reported relative to TMS incorporated as an internal standard ($\delta = 0$ ppm for both ^{1}H and ^{13}C). General NMR experimental details for 1D ^{1}H, ^{13}C, and DEPT and standard gradient-selected 2D DQF-COSY, HSQC, HMBC, and long-range COSY spectra have been previously described.[1] NOE contacts were provided by 1D NOESY[2] spectra using a 50 ms Gaussian-shaped pulse for selective excitation and a mixing time of 0.5 s. Spin analysis was performed using Perch[3] iteration software for the extraction of δ_H and $J_{H,H}$. Chiral NMR included the use of a chiral derivatizing agent (CDA, Mosher's method[4]) and the use of (*S*)-(−)-ethyl lactate and the enantiomers (*R*)-(+)- and (*S*)-(−)-1-phenylethylamine as chiral solvating agents (CSAs) to effect enantiodifferentiation or to better resolve the stereoisomers.[5] Selected spectra (^{1}H, ^{13}C, HSQC, and HMBC) for alnumycin A1 (**1**) and prealnumycin (**2**) are presented in Fig.s ESI18–26.

Molecular modeling: geometry optimization, vibrational analysis, thermochemistry, electronic circular dichroism (ECD), and optical rotation (OR)

DFT quantum chemical calculations were performed using *Gaussian09*[6] (version A.01) and analyzed using GUIs *GaussView* (versions 3.07 and 5.0.8) and *GaussSum*[7] (version 2.2). Structures were first geometry-optimized using the M06-2X hybrid meta density functional[8] with the 6-31G(d) basis set followed by vibrational analysis and thermochemistry calculations (and invoking the keyword *freq=noraman*) at the same level of theory conducted to confirm that the optimized structures were true minima on the potential energy surface by not providing imaginary frequencies and to obtain the thermodynamic contributions at 298.15 K wherein frequencies were left unscaled. Calculations were performed in the gas phase and the optimized structures are depicted in Fig.s ESI4–17 followed by their atomic coordinates. IR frequencies, thermochemistry, and OR[9] properties were calculated for the optimized structures at the same level of theory in the gas phase. The calculated OR, all at $\lambda = 589.3$ nm (except for **2** where a range of values 375–1,200 nm were calculated), are given in the figure captions of the optimized structures.

For prealnumycin (**2**), two stable conformers were found, one with an axially orientated *n*-propyl group and the other with it equatorially orientated, from free-hand formulated starting structures. The conformer with the axially orientated *n*-propyl group was 4.40 kcal/mol lower in energy than the equatorially orientated *n*-propyl group and hence only it was subsequently used as a starting unit for construction of the *S* enantiomer of **2** {and consequently for the construction of the C-1 epimer of alnumycin A1α (**1α**)}, **1α**, and **1β**. For construction of the C-1 epimer of **1α**, **1α**, and **1β**, unsubstituted 1,3-dioxane units for both enantiomers in chair conformations were first constructed by hand and optimized prior to attachment to the prealnumycin unit. Once constructed, various orientations about the

C_8–$C_{1'}$ bond were optimized resulting in three stable conformations, two of which were essentially equal in energy, for **1α**, **1β**, and the C-1 epimer of **1α**.

ECD[10] spectra were calculated using time-dependent DFT (TD-DFT) at the M06-2X/6-311+G(d) level of theory and were found to be sufficiently modeled for bands located at wavelengths longer than 200 nm (the experimental cut off for methanol) using 24 excited states with only minimal improvement occurring for these bands when more than 24 excited states were used; inclusion of a solvent model and expansion of the basis set were also evaluated but were not found to sufficiently increase the fidelity of the results to warrant usage. Spectra were calculated for the two low-energy conformers of alnumycin A1α (**1α**) and A1β (**1β**) and for both conformers of prealnumycin (**2**); for **1α** and **1β**, population-weighted average spectra[11] based on their predicted Boltzmann distributions were produced from the individual spectra by proportionate addition of the intensities at each frequency with a final spectrum for **1** produced by similar proportionate addition of these resultant intensities using the measured ratio of **β**:**α** (3:2) taken from a ^{1}H NMR spectrum. The calculated ECD spectra are depicted in Fig.s 3, ESI2, and ESI3.

UV-vis spectroscopy, ECD, and OR

UV-vis spectra were acquired on a GeneQuant 1300 (GE Healthcare) spectrophotometer equipped with a DAD and a 1 cm pathlength cell. Samples in methanol solution were scanned from 250–650 nm in 1 nm steps. Optical rotations were measured at 22 °C using a Jasco DIP-360 polarimeter equipped with a 1 dm pathlength cell and the sodium D lines (589.3 nm) for samples made up to a concentration of 25 μg/mL in methanol. ECD spectra were measured over the range of 200–650 nm at 25 °C using a Chirascan™ circular dichroism spectrometer equipped with a 1 cm pathlength cell for samples made up to a concentration of 50 μg/mL in methanol (**1** and **2**) or acetonitrile (**2**).

Mass spectrometry

A Bruker micrOTOFQ mass spectrometer was used for the measurement of high resolution mass spectra for **1** under ESI$^-$ mode using the following conditions: mass range, 100–3000 amu; capillary voltage, +4,000 V; end plate offset voltage,−500 V; nebulizer pressure, 1.6 bar; drying gas flow rate, 12.0 L/min; drying heater temperature, 200 °C. Samples were introduced to the ESI source by coupling to an Agilent Technologies 1200 Series HPLC equipped with a diode array detector and a SunFire C18 column (150 × 2.1 mm, 3.5 μm particle size, Waters) developed with gradient elution from 0.1% formic acid in 15% acetonitrile to 100% acetonitrile. A VG ZabSpec-oa-TOF mass spectrometer was used for the measurement of high resolution mass spectra under EI$^+$ mode at 70 eV for **2**.[12]

Chromatography: TLC, column chromatography, and HPLC

For TLC, silica gel 60 F_{254} backed on glass plates or aluminium sheets were used eluted with, in general, hexane–isopropanol, 7:3 or 1:1, amongst other solvent systems. For column chromatography, silica gel (particle size 0.040–0.063 mm, Merck) was used eluted with, in general, hexane–isopropanol, 7:3 or 1:1,

amongst other solvent systems. Analytical RP-HPLC consisted of a SCL-10Avp (Shimadzu) system equipped with a UV-vis DAD and a LiChroCART 250-4 RP-18 Lichrospher 100 column (250 × 4 mm, 5 μm particle size, Merck) eluted with 20 mM aqueous ammonium acetate and a 55–100% acetonitrile gradient (optimized conditions). Semi-preparative RP-HPLC consisted of a L-6200A (Merck Hitachi) system equipped with a UV-vis DAD and a LiChroCART 250-10 RP-18 Lichrospher 100 column (250 × 10 mm, 10 μm particle size, Merck) eluted with gradients as *per* the analytical system.

Microbial growth and conditions and extraction of metabolites

Alnumycin A1 (**1**)-producing *Streptomyces* sp. CM020 strain was obtained from Galilaeus Oy (Kaarina, Finland). Prealnumycin (**2**)-producing *Streptomyces albus*/pAoriΔind double mutant strain was generated by inactivation of the overlapping open reading frames *alnB* and *alnA* on the cosmid pAlnuori as described earlier.[12] For production of the metabolites, bacterial strains were cultivated in Erlenmeyer flasks in modified E1 medium[13] (whereby Pharmamedia was replaced by soy flour and starch was not included) for 5 days at 300 rpm, 301 K. Amberlite XAD-7 (1 g/50 mL) was added for adsorption of the metabolites from the cultivation medium. At the end of cultivation, the resin was separated by the repeated addition of tapwater and decanting. Desorption of the metabolites was effected with isopropanol.

Reaction with Mosher's reagent[4]

To prepare the (*tris*-)*S*-MTP derivatives of prealnumycin (**2**) and alnumycin A1 (**1**), *i.e.* the products obtained from reaction with *R* Mosher's chloride (MTP), 2 mg of **2** (or for **1**, *ca.* 0.05 mg) in 200 μL of $CDCl_3$ (400 μL of $CDCl_3$ dried over 4 Å molecular sieves) containing TMS as reference was placed in an NMR tube followed by 500 μL (100 μL) of d_5-pyridine dried over 4 Å molecular sieves and 20 μL (3 μL) of (*R*)-α-methoxy-α-trifluorophenylacetyl chloride. The solution was thoroughly mixed and left to stand overnight prior to measuring the ^{1}H NMR spectrum (or alternatively analyzed within tens of minutes; if the reaction was incomplete, it was left to finish in the NMR spectrometer). The *R*-MTP derivative of **2** was prepared using (*S*)-α-methoxy-α-trifluorophenylacetyl chloride under otherwise identical conditions.

Alnumycin A1 (1)

From the crude culture extract, alnumycin A1 (**1**) was first obtained by column chromatography over silica gel (eluent hexane–isopropanol, 7:3); to obtain a highly purified sample of **1**, the fraction containing it was subjected to repeated semi-preparative RP-HPLC. Numerous chromatographic attempts with varying conditions, including the addition of a chiral mediator (*S*)-(−)-ethyl lactate, were tried to effect the separation of the C-1 inverse-epimeric pairs **1α** and **1β** but were unsuccessful. For **1**: $[\alpha]^{22}_{D}$, +855° (*c* 0.0025, methanol). ESI$^-$HRMS: *m*/*z*, 415.1387; calculated for $C_{22}H_{23}O_8$, 415.1398. The ^{1}H and ^{13}C NMR data for **1α** and **1β** are presented in Table ESI1 with selected spectra (^{1}H, ^{13}C, HSQC, and HMBC) for **1** presented in Fig.s ESI18–22. The UV-vis spectra for **1** are presented in Fig. ESI1; λ_{max}, 301 and 470 nm. The experimental and calculated ECD spectra for **1** are presented in Fig. ESI3.

Prealnumycin (2)

Prealnumycin (**2**) was obtained from a crude extract containing predominantly only **2** by column chromatography over silica gel (eluent hexane–isopropanol, 1:1). For a highly purified sample of **2**, a fraction highly enriched in **2** was subjected to semi-preparative RP-HPLC. EI^+-HRMS: *m*/*z*, 284.1055; calculated for $C_{17}H_{16}O_4$, 284.1049.[12] The ^1H and ^{13}C NMR data are presented in Table ESI1 with selected spectra (^1H, ^{13}C, HSQC, and HMBC) for **2** presented in Fig.s ESI23–26. The UV-vis spectrum is presented in Fig. ESI1; for **2**: λ_{max}, 299 and 460 nm. The ECD spectra are presented in Fig.s 3 ESI2 (calculated) and ESI3 (calculated and experimental).

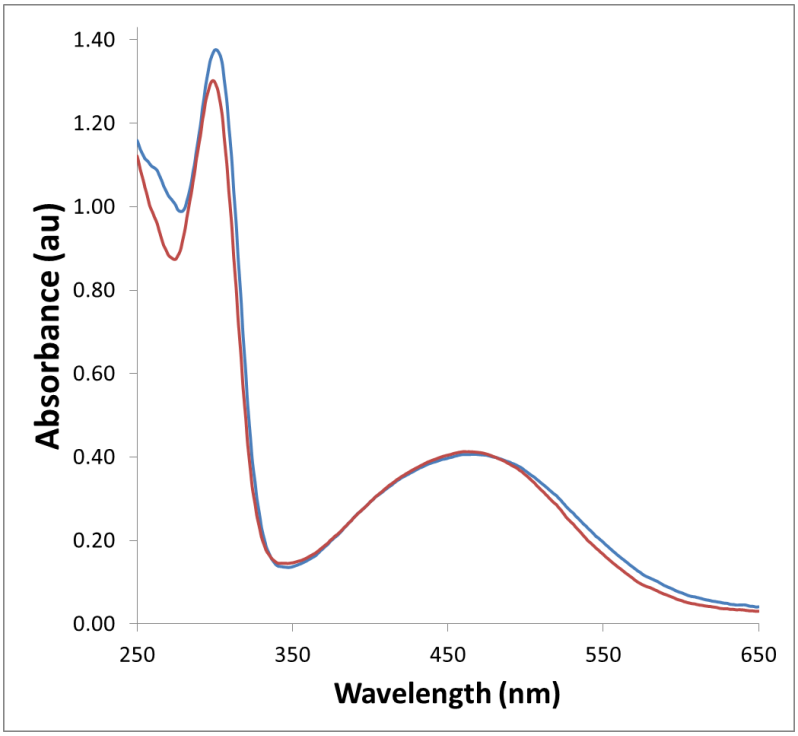

Fig. ESI1 UV-vis spectra of — alnumycin A1 (**1**) and — prealnumycin (**2**) in CH_3OH.

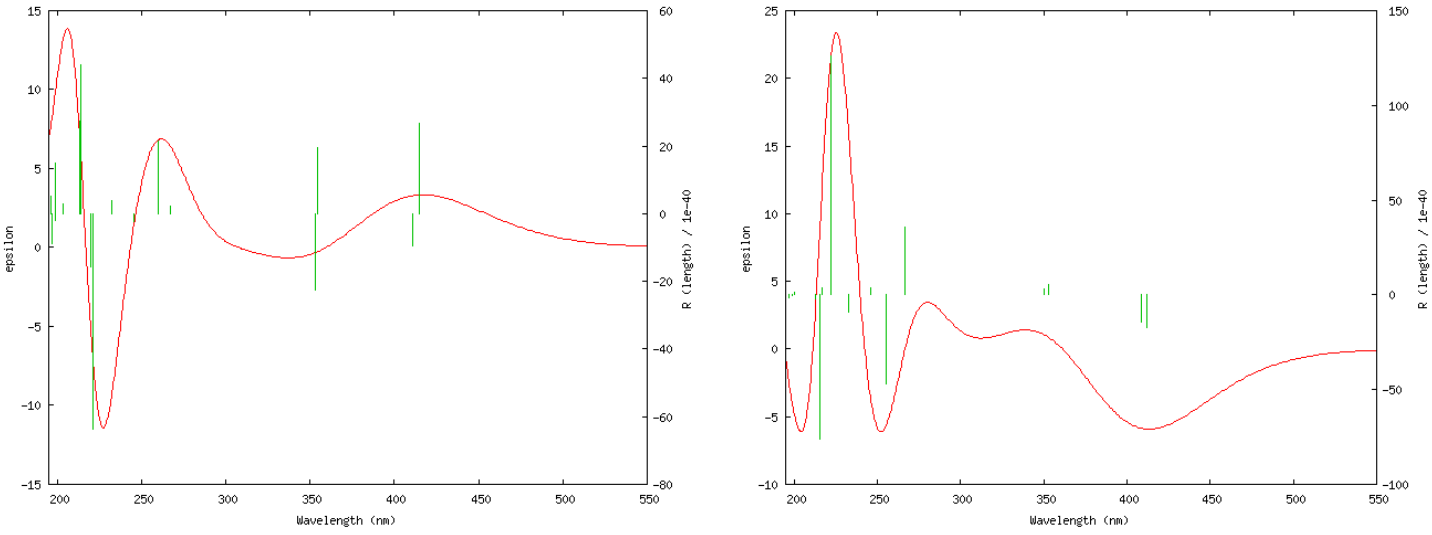

Fig. ESI2 Calculated ECD spectra of (*R*)-prealnumycin (**2**) with an axial *n*-propyl group (left; Δ*G*, 0.00 kcal/mol) and with an equatorial *n*-propyl group (right; Δ*G*, +4.40 kcal/mol). Computed at the M06-2X/6-311G+(d) level of theory in the gas phase with 24 excited states.

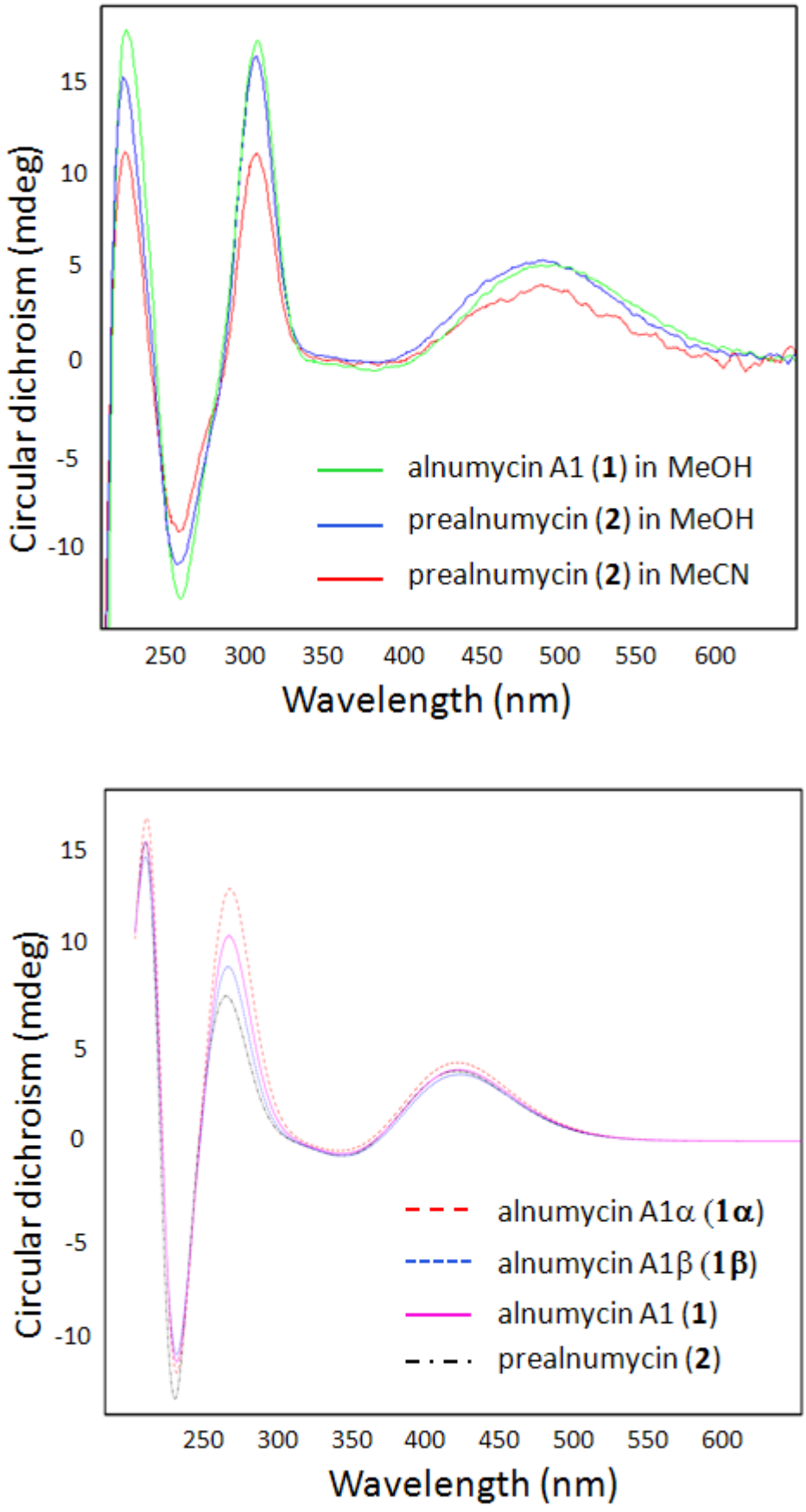

Fig. ESI3 Observed (top) and calculated (bottom) ECD spectra of alnumycin A1 (**1**) and (*R*)-prealnumycin (**2**). The calculated spectra of **1α** and **1β** represent Boltzmann-calculated population-weighted averages[11] of two low-energy conformers whilst **1** represents an average of **1β** and **1α** based on a ratio of 3:2, respectively, as measured by ^{1}H NMR. Computations performed at the M06-2X/6-311G+(d) level of theory in the gas phase with 24 excited states. This is an enlarged reproduction of Fig. 3.

Table ESI1 ^{1}H and ^{13}C NMR data of alnumycins A1α (**1α**) and A1β (**1β**) and prealnumycin (**2**) in $CDCl_3$ at 25 °C

atom	alnumycin A1β (**1β**), major isomer			alnumycin A1α (**1α**), minor isomer			prealnumycin (**2**)		
	δ/ppm		multiplicity; *J*/Hz (spin partner)	δ/ppm		multiplicity; *J*/Hz (spin partner)	δ/ppm		multiplicity; *J*/Hz (spin partner)
	δ_C	δ_H		δ_C	δ_H		δ_C	δ_H	
1	73.009	5.637	app dd; 9.41 (H-11a), 3.51 (H-11b);	73.007	5.623	app dd; 9.34 (H-11a), 3.52 (H-11b)	72.98	5.651	app dd; 9.35 (H-11a), 3.52 (H-11b), 0.41 (H-5)
3	158.61	–	–	158.62	–	–	158.44	–	–
4	100.010	5.595	qt; −0.87 (H-14)	100.014	5.593	qt; −0.90 (H-14)	100.02	5.610	qt d; −0.87 (H-14), −0.27 (H-5)
4a	139.708	–	–	139.706	–	–	139.55	–	–
5	114.45	7.111	s	114.45	7.106	s	114.50	7.137	br t; 0.41 (H-1), −0.27 (H-4)
5a	131.27	–	–	131.26	–	–	131.25	–	–
6	184.76	–	–	184.76	–	–	184.61	–	–
7	135.61	7.0715	ol d; −0.89 (H-1')	135.61	7.0705	ol d; −0.90 (H-1')	138.92	6.849	d_{AB}; 10.26 (H-8)
8	144.31	–	–	144.32	–	–	139.12	6.877	d_{AB}; 10.26 (H-7)
9	186.92	–	–	186.90	–	–	188.87	–	–
9a	112.87	–	–	112.85	–	–	112.96	–	–
10	157.10	12.160	s	157.09	12.149	s	156.87	12.180	s
10a	122.47	–	–	122.46	–	–	122.33	–	–
11	34.87	a, 1.99 b, 1.52	m; m	34.85	a, 1.99 b, 1.52	m; m	34.91	a, 2.01 b, 1.54	m; m
12	18.14	a, 1.54 b, 1.47	m; m	18.12	a, 1.54 b, 1.47	m; m	18.15	a, 1.55 b, 1.49	m; m
13	13.80	0.960	app t; 7.13 (H-12 × 2)	13.79	0.955	app t; 7.14 (H-12 × 2)	13.79	0.966	app t; 7.15 (H-12 × 2)
14	20.43	1.9619	d; −0.87 (H-4)	20.44	1.9615	d; −0.90 (H-4)	20.44	1.966	d; −0.87 (H-4)
1'	93.98	5.708	ol d; −0.89 (H-7)	93.97	5.710	ol d; −0.90 (H-7)	–	–	–
3'	70.93	equat. 4.309; axial, 3.650	dd; −10.90 (H-3'ax), 5.42 (H-4') t; −10.90 (H-3'eq), 10.30 (H-4')	70.94	equat. 4.303; axial, 3.651	dd; −10.87 (H-3'ax), 5.41 (H-4'); t; −10.87 (H-3'eq), 10.23 (H-4')	–	–	–
4'	62.47	3.89–3.98	ol m (2 × H-4', 4 × H-6')	62.46	3.89–3.98	ol m (2 × H-4', 4 × H-6')	–	–	–
5'	81.45	3.736	dt; 9.29 ((H-4'), 4.41 (H-6'a), 4.01 (H-6'b)	81.47	3.739	dt; 9.26 ((H-4'), 4.33 (H-6'a), 4.08 (H-6'b)	–	–	–
6'	62.63	3.89–3.98	ol m (2 × H-4', 4 × H-6')	62.61	3.89–3.98	ol m (2 × H-4', 4 × H-6')	–	–	–

Legend: app, apparent; br, broad or broadened; $d_{(AB)}$, doublet (AB character); m, multiplet; ol, overlapped; qt, quartet; s, singlet; t, triplet. [a] Stereoisomer assignments based on Tatsuta.[14]

With reference to Table ESI1, clearly the spectra of the inverse epimeric pair alnumycin A1 (**1α** and **1β**) are extremely similar. For example, the ^{1}H signals for H-1, H-5, and the equatorial H-3' were the only ones for which clear disparity could be observed (heavily overlapped multiplets notwithstanding). The two H-3's were interesting in that for one signal, the presence of two stereoisomers was evident whilst for the other it was not despite the quite fine linewidth of the axial H-3' signal. For the ^{13}C NMR spectrum of **1**, application of an exponential line broadening equating to 2 Hz yielded only the one set of signals; Fourier transformation of the ^{13}C NMR FID for **1** was thereby duly performed without exponential line broadening being applied.

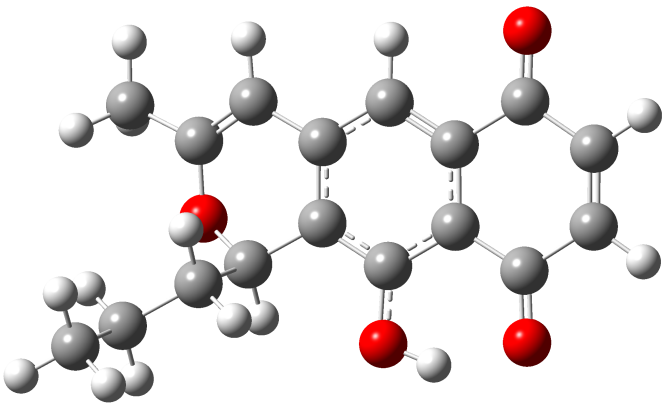

Fig. ESI4 The structure of (*R*)-prealnumycin (**2**) with an axially disposed *n*-propyl group {M06-2X/6-31G(d) level of theory} in the gas phase; ΔE, 0.00; ΔG, 0.00 kcal/mol; $[\alpha]^{25}_{calc}$ (λ, nm):−2,859 ° (375), +1,142° (500), +722° (550), +553° (589.3, D), +518° (600), +380° (660), +319° (700), +165° (900), +85° (1,200).

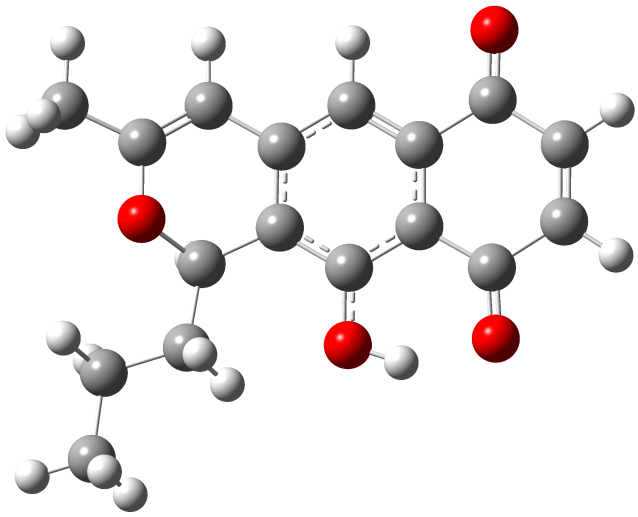

Fig. ESI5 The structure of (*R*)-prealnumycin (**2**) with an equatorially disposed *n*-propyl group {M06-2X/6-31G(d) level of theory} in the gas phase; ΔE, 4.07; ΔG, 4.40 kcal/mol; $[\alpha]^{25}_{D, calc}$ −516°.

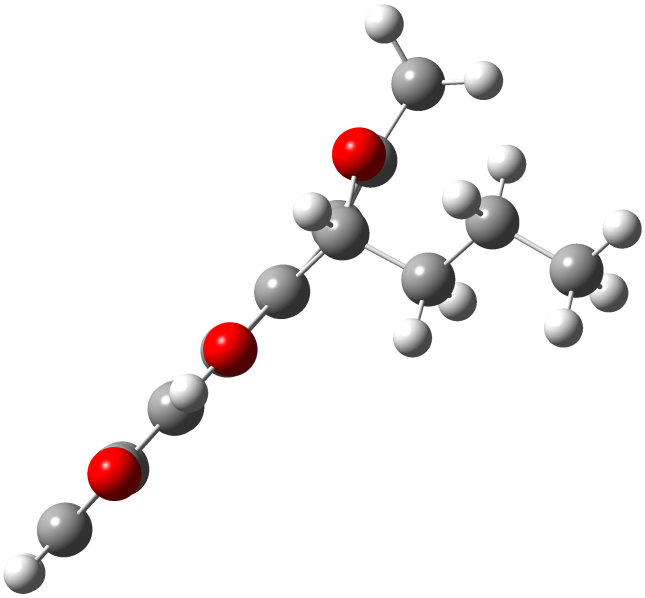

Fig. ESI6 The structure of (*R*)-prealnumycin (**2**) with an axially disposed *n*-propyl group {M06-2X/6-31G(d) level of theory} in the gas phase; ΔE, 0.00; ΔG, 0.00 kcal/mol; $[\alpha]^{25}_{D, calc}$ +553°; side view aspect.

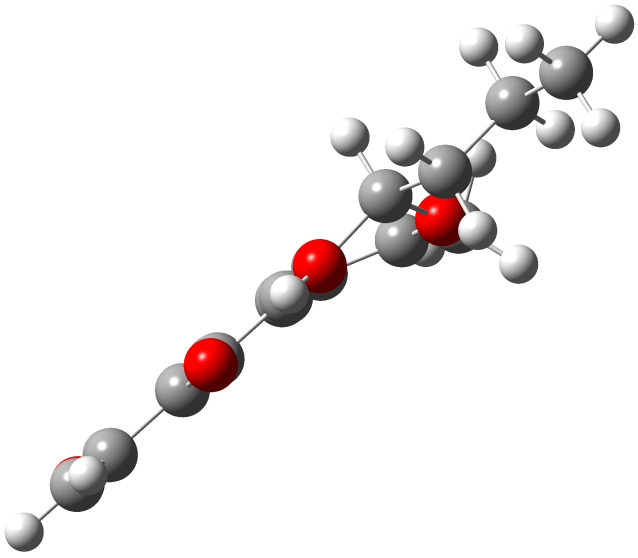

Fig. ESI7 The structure of (*R*)-prealnumycin (**2**) with an equatorially disposed *n*-propyl group {M06-2X/6-31G(d) level of theory} in the gas phase; ΔE, 4.07; ΔG, 4.40 kcal/mol; $[\alpha]^{25}_{D, calc}$ −516°; side view aspect.

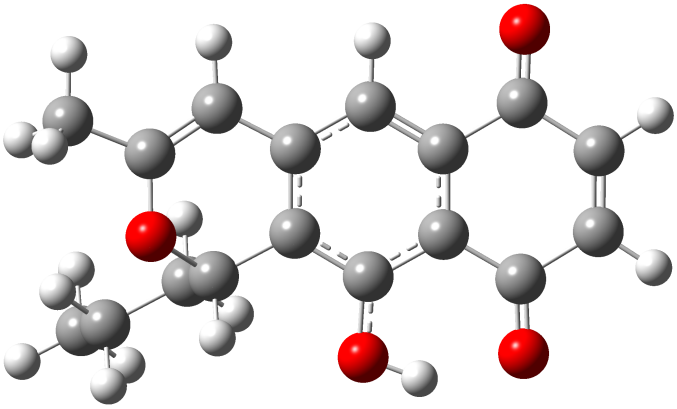

Fig. ESI8 The structure of the *S* enantiomer of **2** with an axially disposed *n*-propyl group {M06-2X/6-31G(d) level of theory} in the gas phase; ΔE, 0.00; ΔG, 0.01 kcal/mol.

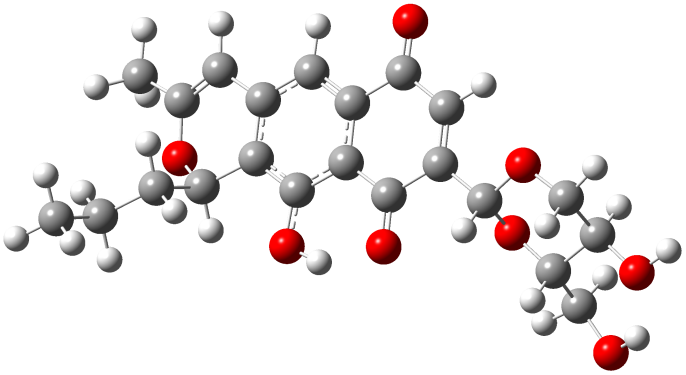

Fig. ESI9 The structure of alnumycin A1α (**1α**), first conformer {M06-2X/6-31G(d) level of theory} in the gas phase; ΔE, 0.06; ΔG, 0.00 kcal/mol; $[\alpha]^{25}_{D,\,calc}$ +640°.

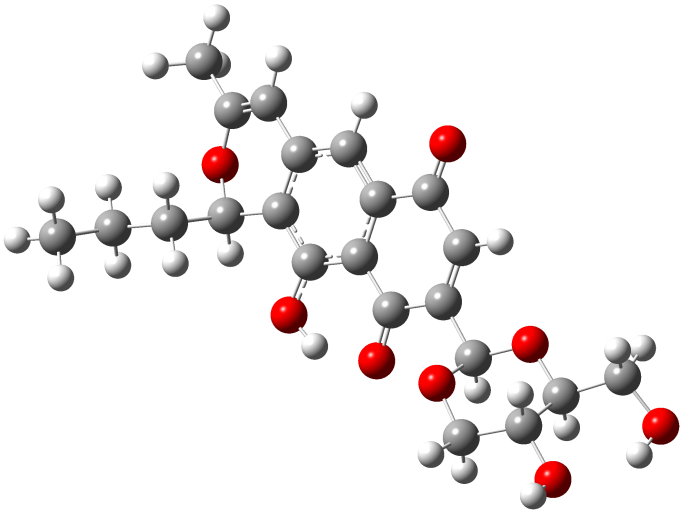

Fig. ESI10 The structure of alnumycin A1α (**1α**), second conformer {M06-2X/6-31G(d) level of theory} in the gas phase; ΔE, 0.00; ΔG, 0.15 kcal/mol; $[\alpha]^{25}_{D,\,calc}$ +392°.

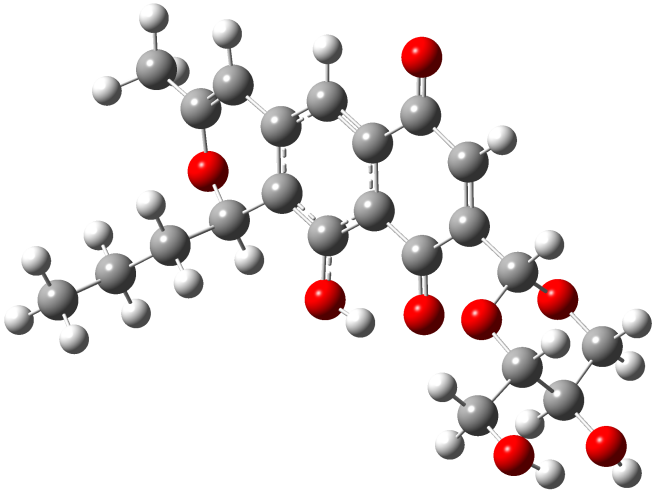

Fig. ESI11 The structure of alnumycin A1α (**1α**), third conformer {M06-2X/6-31G(d) level of theory} in the gas phase; ΔE, 2.55; ΔG, 3.45 kcal/mol; $[\alpha]^{25}_{D,\,calc}$ +304°.

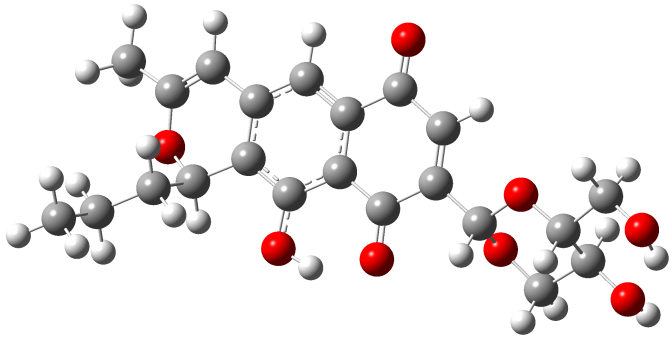

Fig. ESI12 The structure of alnumycin A1β (**1β**), first conformer {M06-2X/6-31G(d) level of theory} in the gas phase; Δ*E*, 0.00; Δ*G*, 0.00 kcal/mol; $[\alpha]^{25}_{D,\,calc}$ +598°.

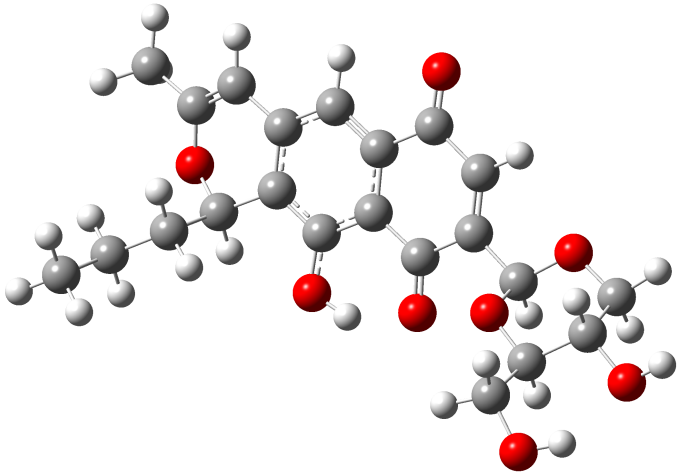

Fig. ESI13 The structure of alnumycin A1β (**1β**), second conformer {M06-2X/6-31G(d) level of theory} in the gas phase; Δ*E*, 0.11; Δ*G*, 0.06 kcal/mol; $[\alpha]^{25}_{D,\,calc}$ +274°.

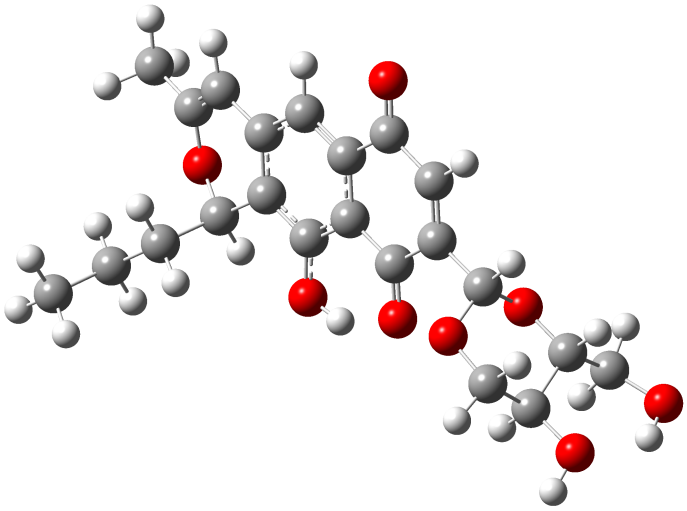

Fig. ESI14 The structure of alnumycin A1β (**1β**), third conformer {M06-2X/6-31G(d) level of theory} in the gas phase; Δ*E*, 2.76; Δ*G*, 3.07 kcal/mol; $[\alpha]^{25}_{D,\,calc}$ +554°.

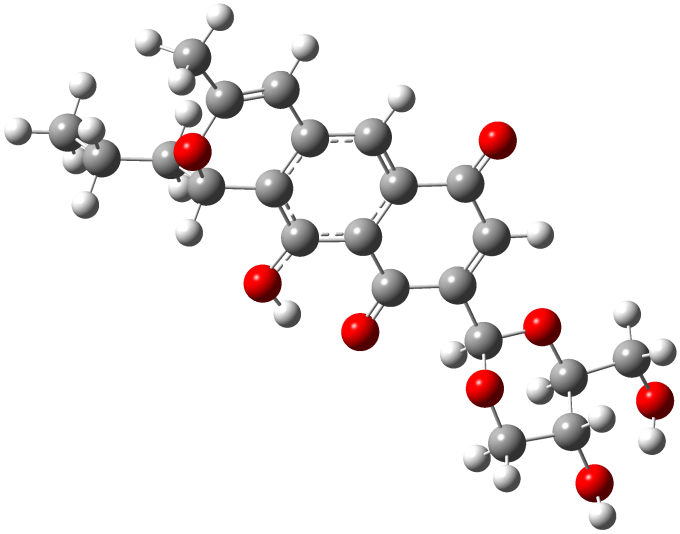

Fig. ESI15 The structure of the C-1 epimer of **1α** (configuration 1*S*,1'*R*,4'*R*,5'*S*), first conformer {M06-2X/6-31G(d) level of theory} in the gas phase; Δ*E*, 0.00; Δ*G*, 0.00 kcal/mol; $[\alpha]^{25}_{D,\,calc}$ −598°.

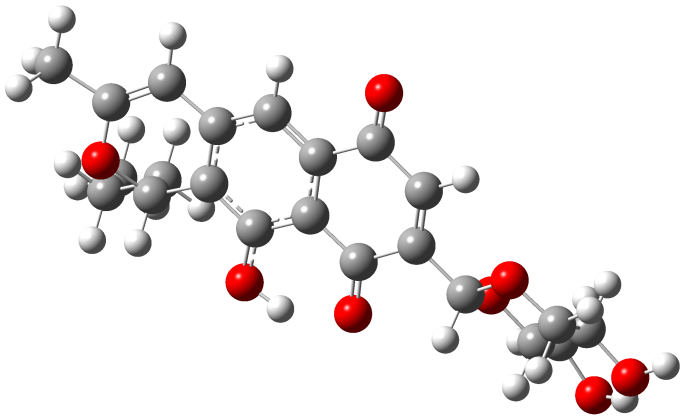

Fig. ESI16 The structure of the C-1 epimer of **1α** (configuration 1*S*,1'*R*,4'*R*,5'*S*), second conformer {M06-2X/6-31G(d) level of theory} in the gas phase; Δ*E*, 0.11; Δ*G*, 0.06 kcal/mol; $[\alpha]^{25}_{D,\,calc}$ −274°.

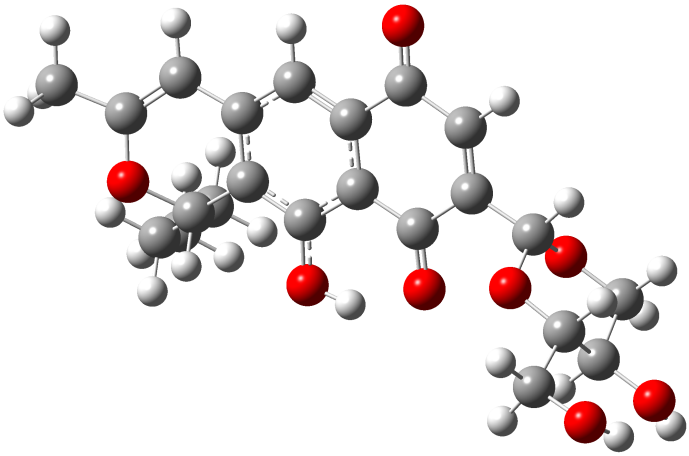

Fig. ESI17 The structure of the C-1 epimer of **1α** (configuration 1*S*,1'*R*,4'*R*,5'*S*), third conformer {M06-2X/6-31G(d) level of theory} in the gas phase; Δ*E*, 2.76; Δ*G*, 3.08 kcal/mol; $[\alpha]^{25}_{D,\,calc}$ −554°.

Atomic structure Cartesian coordinates of the modeled structures:

Fig. ESI4:

Fig. ESI5:

Fig. ESI6:
see Fig. ESI4.

Fig. ESI7:
see Fig. ESI5.

Fig. ESI8:

Fig. ESI9:

Fig. ESI10:

Fig. ESI11:

Fig. ESI12:

Fig. ESI13:

Fig. ESI14:

Fig. ESI15:

Fig. ESI16:

Fig. ESI17:

References

1 (*a*) J. Mäki, P. Tähtinen, L. Kronberg and K. D. Klika, *J. Phys. Org. Chem.*, 2005, **18**, 240; (*b*) P. Virta, A. Koch, M. U. Roslund, P. Mattjus, E. Kleinpeter, L. Kronberg, R. Sjöholm and K. D. Klika, *Org. Biomol. Chem.*, 2005, **3**, 2924; (*c*) K. D. Klika, J. Bernát, J. Imrich, I. Chomča, R. Sillanpää and K. Pihlaja, *J. Org. Chem.*, 2001, **66**, 4416; (*d*) E. Balentová, J. Imrich, J. Bernát, L. Suchá, M. Vilková, N. Prónayová, P. Kristian, K. Pihlaja and K. D. Klika, *J. Heterocycl. Chem.*, 2006, **43**, 645.

2 (*a*) J. Stonehouse, P. Adell, J. Keeler and A. J. Shaka, *J. Am. Chem. Soc.*, 1994, **116**, 6037; (*b*) K. Stott, J. Stonehouse, J. Keeler, T. L. Hwang and A. J. Shaka, *J. Am. Chem. Soc.*, 1995, **117**, 4199.

3 See, for example: R. Laatikainen, M. Niemitz, U. Weber, J. Sundelin, T. Hassinen and J. Vepsäläinen, *J. Magn. Reson. Ser. A*, 1996, **120**, 1. See also Peak Research NMR Software; Perch Solutions, Ltd.: Kuopio, Finland, 2003 (website: http://www.perchsolutions.com).

4 (*a*) J. A. Dale and H. S. Mosher, *J. Am. Chem. Soc.*, 1973, **95**, 512; (*b*) J. A. Dale, D. L. Dull and H. S. Mosher, *J. Org. Chem.*, 1969, **34**, 2543.

5 (*a*) K. D. Klika, M. Budovská and P. Kutschy, *J. Fluor. Chem.*, 2010, **131**, 467; (*b*) K. D. Klika, M. Budovská and P. Kutschy, *Tetrahedron: Asymmetry*, 2010, **21**, 647.

6 M. J. Frisch, G. W. Trucks, H. B. Schlegel, G. E. Scuseria, M. A. Robb, J. R. Cheeseman, G. Scalmani, V. Barone, B. Mennucci, G. A. Petersson, H. Nakatsuji, M. Caricato, X. Li, H. P. Hratchian, A. F. Izmaylov, J. Bloino, G. Zheng, J. L. Sonnenberg, M. Hada, M. Ehara, K. Toyota, R. Fukuda, J. Hasegawa, M. Ishida, T. Nakajima, Y. Honda, O. Kitao, H. Nakai, T. Vreven, J. A. Montgomery, Jr., J. E. Peralta, F. Ogliaro, M. Bearpark, J. J. Heyd, E. Brothers, K. N. Kudin, V. N. Staroverov, R. Kobayashi, J. Normand, K. Raghavachari, A. Rendell, J. C. Burant, S. S. Iyengar, J. Tomasi, M. Cossi, N. Rega, J. M. Millam, M. Klene, J. E. Knox, J. B. Cross, V. Bakken, C. Adamo, J. Jaramillo, R. Gomperts, R. E. Stratmann, O. Yazyev, A. J. Austin, R. Cammi, C. Pomelli, J. W. Ochterski, R. L. Martin, K. Morokuma, V. G. Zakrzewski, G. A. Voth, P. Salvador, J. J. Dannenberg, S. Dapprich, A. D. Daniels, O. Farkas, J. B. Foresman, J. V. Ortiz, J. Cioslowski and D. J. Fox, *GAUSSIAN09 (Revision A.01)*, Gaussian, Inc., Wallingford, CT, 2009.

7 N. M. O'Boyle, A. L. Tenderholt and K. M. Langner, *J. Comp. Chem.*, 2008, **29**, 839.

8 (*a*) Y. Zhao and D. G. Truhlar, *Theor. Chem. Acc.*, **2008**, *120*, 215; (*b*) Y. Zhao and D. G. Truhlar, *Acc. Chem. Res.*, 2008, **41**, 157.

9 (*a*) P. J. Stephens, F. J. Devlin, J. R. Cheeseman and M. J. Frisch, *J. Phys. Chem. A*, 2001, **105**, 5356; (*b*) K. Ruud and T. Helgaker, *Chem. Phys. Lett.*, 2002, **352**, 533; (*c*) P. J. Stephens, F. J. Devlin, J. R. Cheeseman, M. J. Frisch and C. Rosini, *Org. Lett.*, 2002, **4**, 4595; (*d*) P. J. Stephens, D. M. McCann, J. R. Cheeseman and M. J. Frisch, *Chirality*, 2005, **17**, S52; (*e*) P. J. Stephens, J. J. Pan, F. J. Devlin and J. R. Cheeseman, *J. Nat. Prod.*, 2008, **71**, 285.

10 (*a*) A. E. Hansen and K. L. Bak, *Enantiomer*, 1999, **4**, 455; (*b*) J. Autschbach, T. Ziegler, S. J. A. van Gisbergen and E. J. Baerends, *J. Chem. Phys.*, 2002, **116**, 6930.

11 Reference 9 in the manuscript.

12 Reference 3 in the manuscript.

13 K. Ylihonko, J. Hakala, J. Niemi, J. Lundell and P. Mäntsälä, *Microbiology*, 1994, **140**, 1359.

14 Reference 2d in the manuscript.

Fig. ESI18 ^{1}H NMR spectrum of alnumycin A1 (**1**).

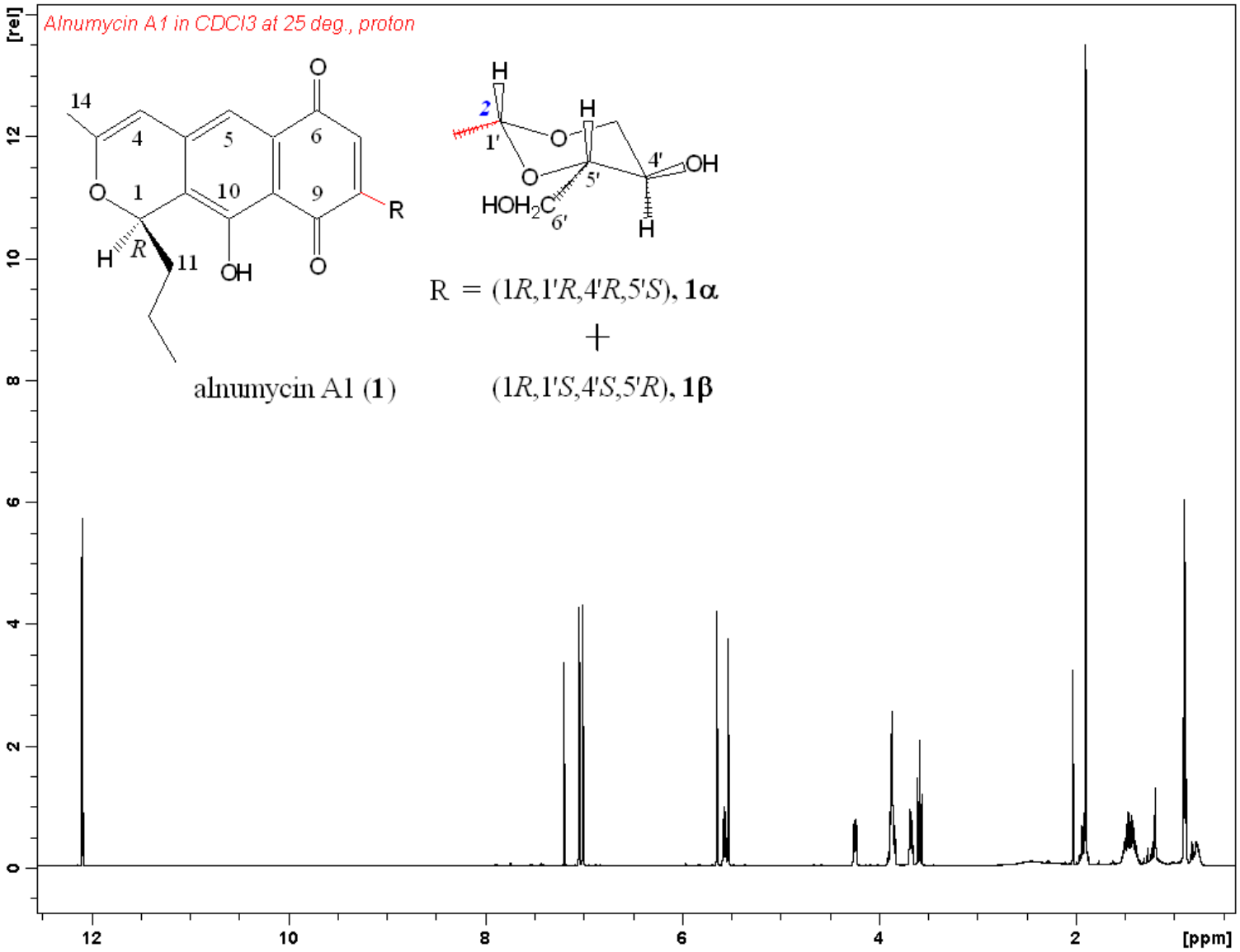

Fig. ESI19 ^{1}H NMR spectrum of alnumycin A1 (**1**), expansion of the region containing the dioxane ring protons.

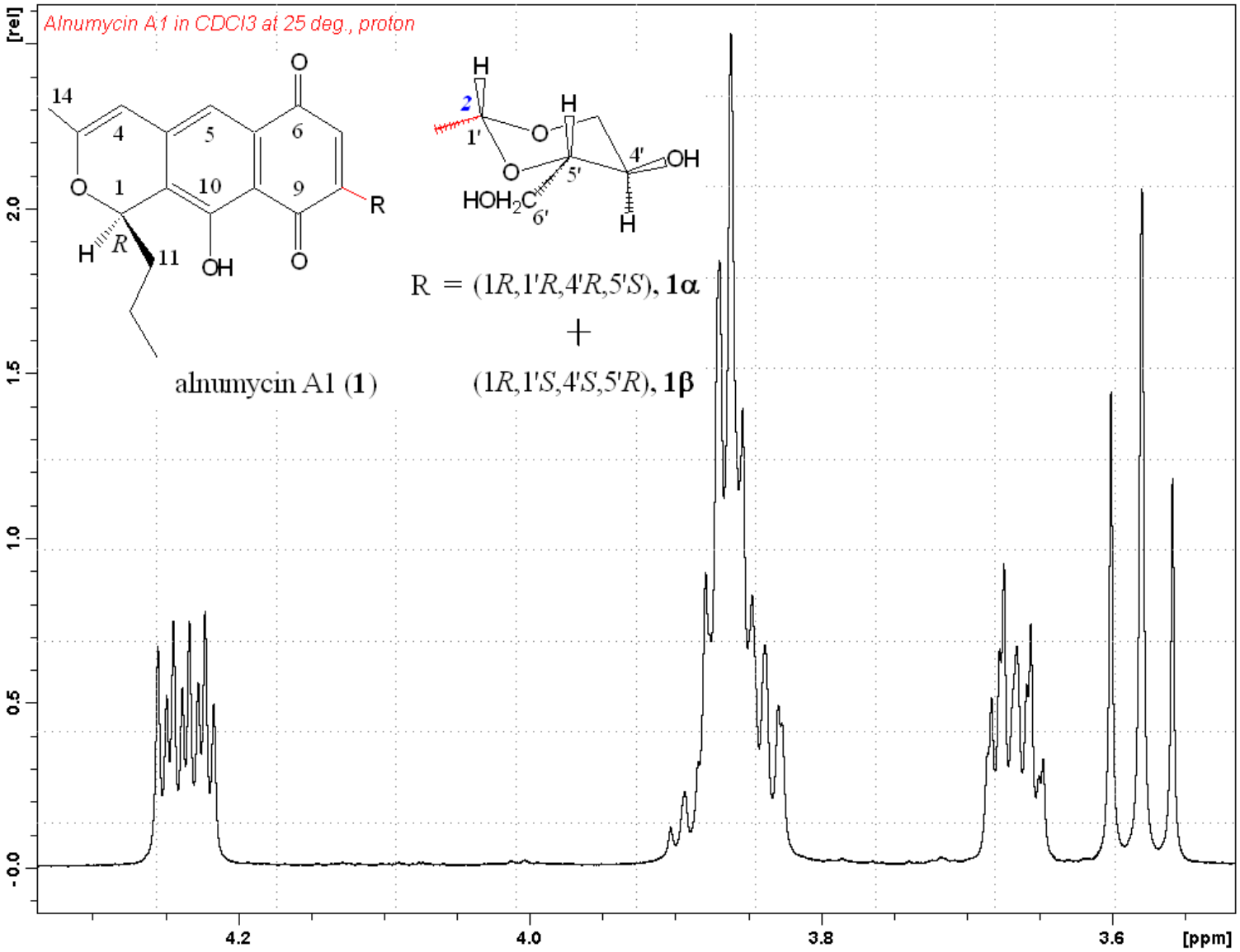

Fig. ESI20 ^{13}C NMR spectrum of alnumycin A1 (**1**).

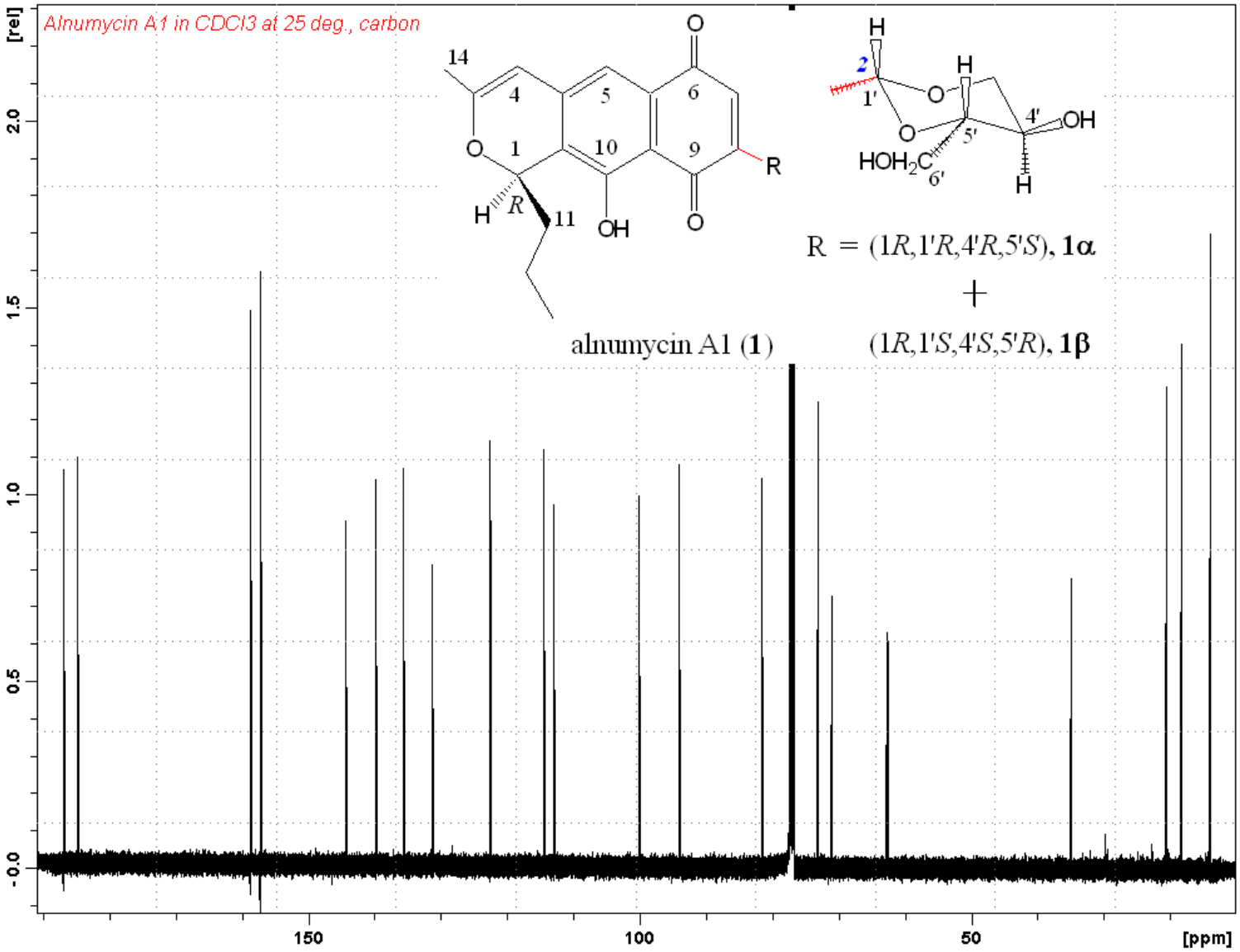

Fig. ESI21 HSQC NMR spectrum of alnumycin A1 (**1**).

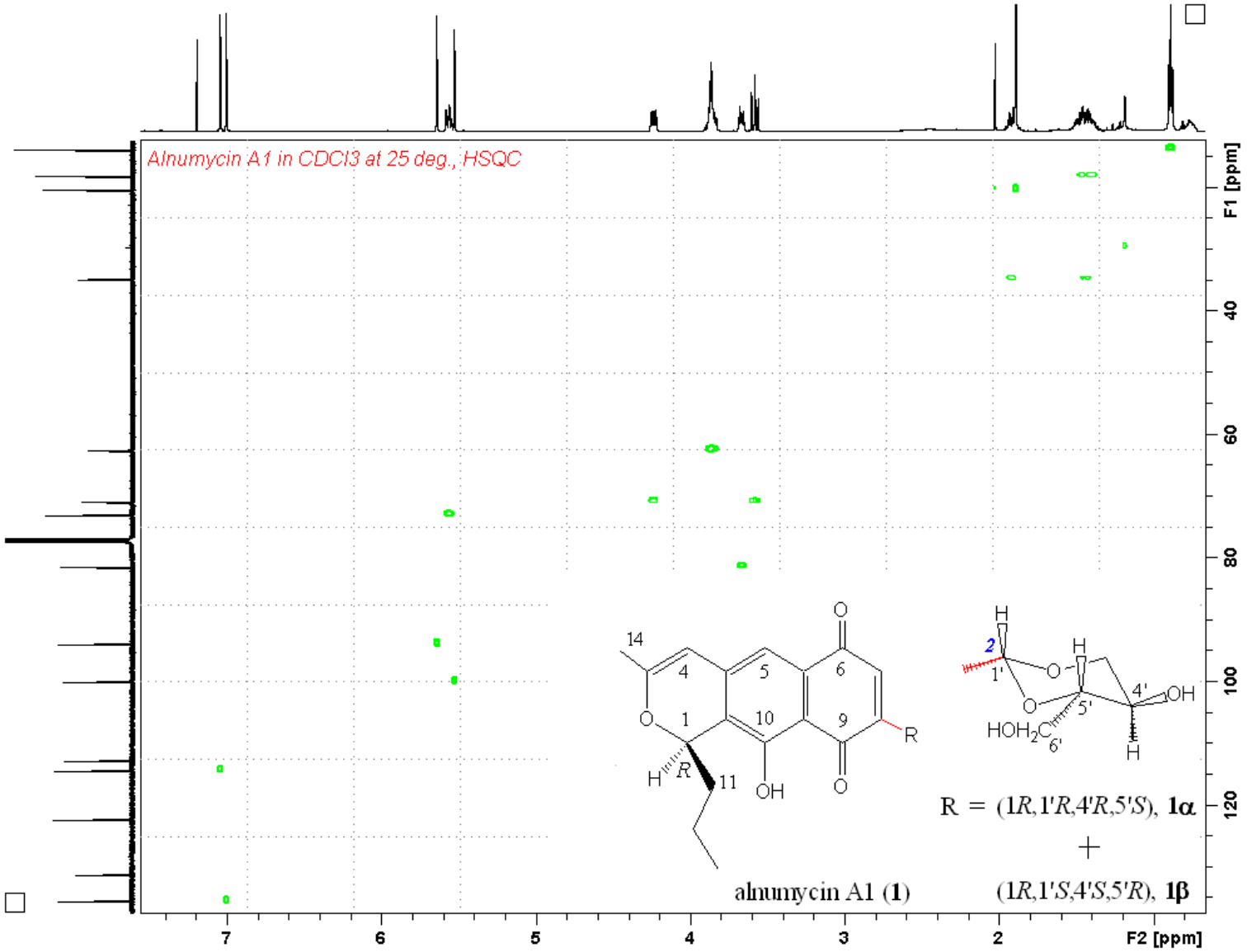

Fig. ESI22 HMBC NMR spectrum of alnumycin A1 (**1**).

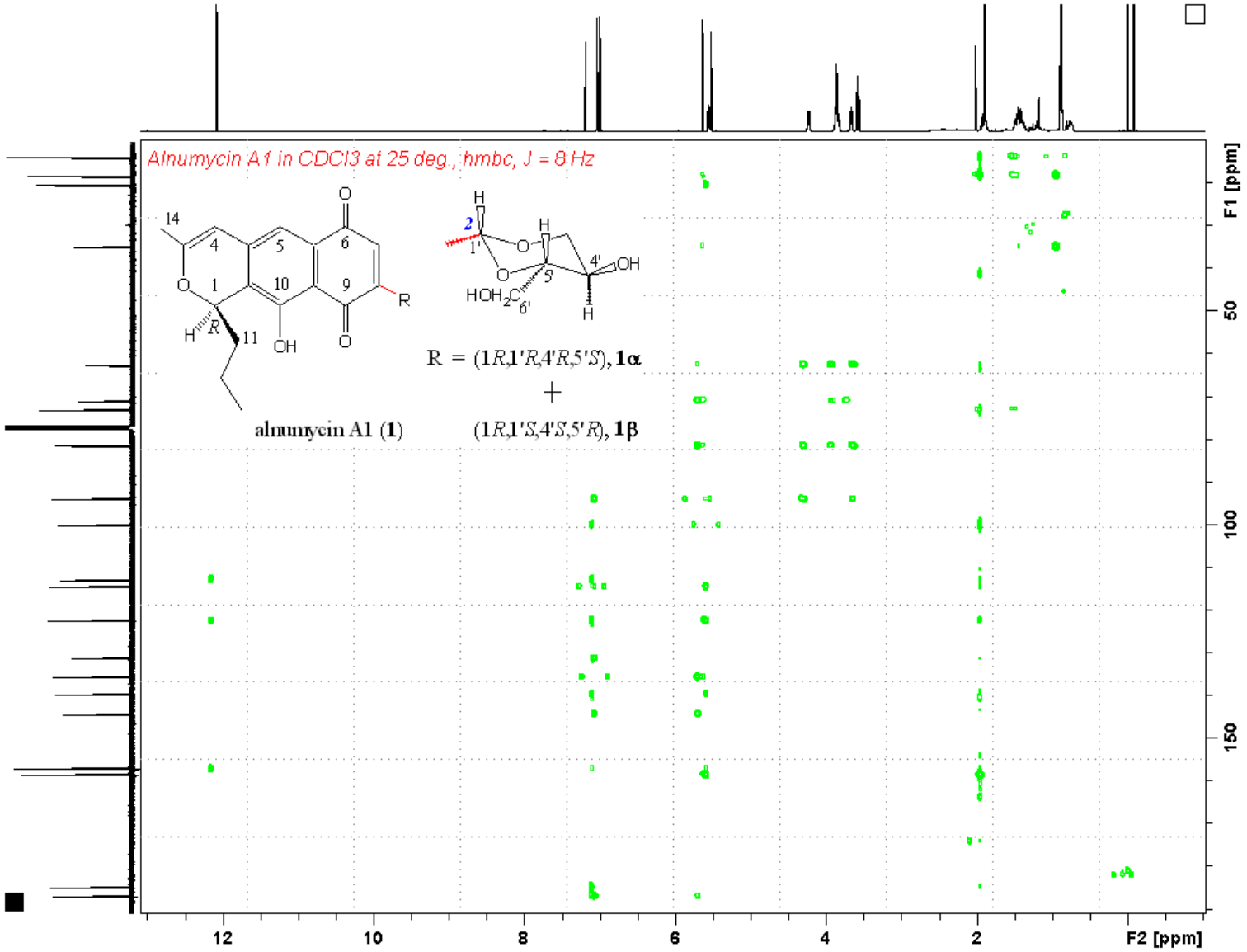

Fig. ESI23 ^{1}H NMR spectrum of prealnumycin (**2**).

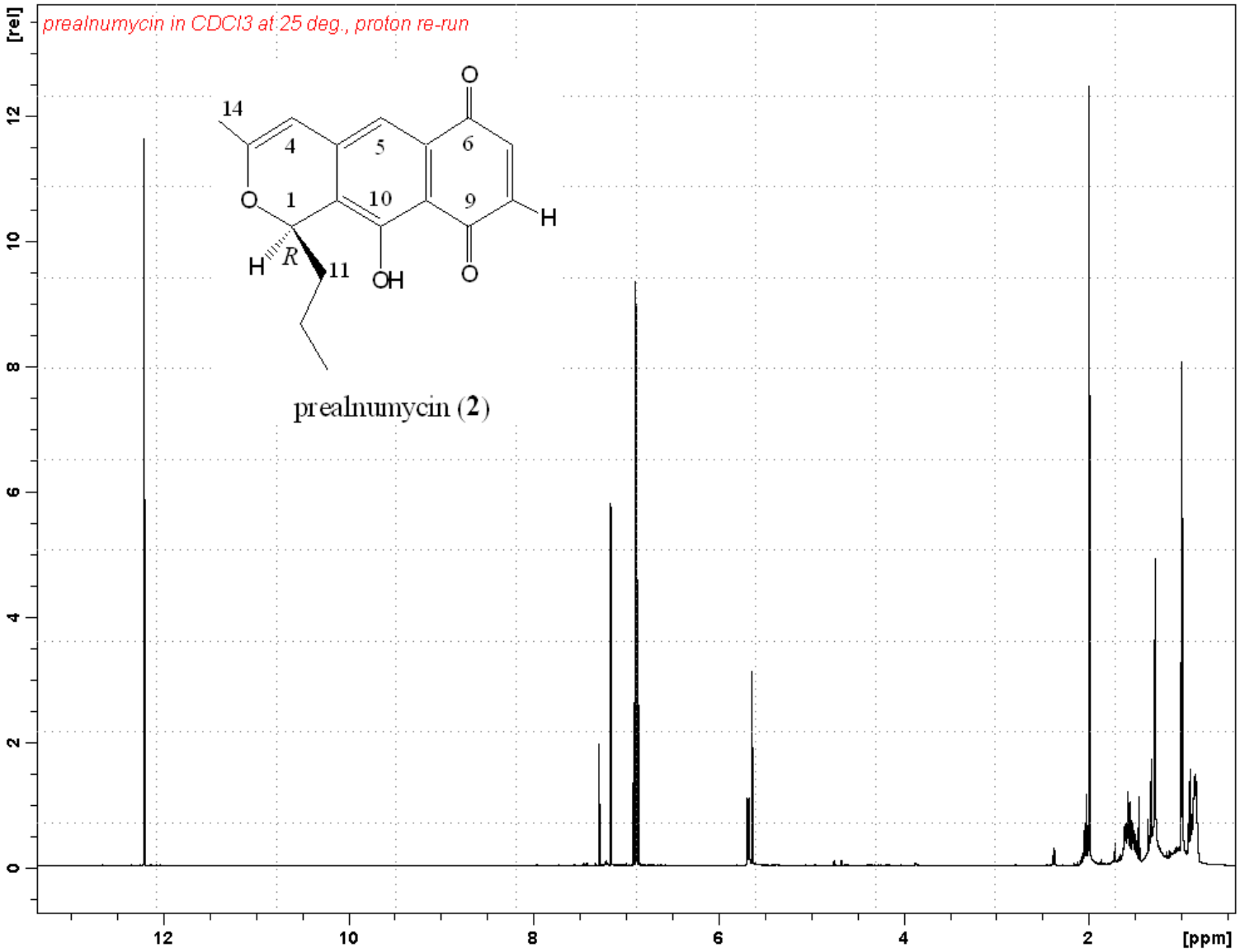

Fig. ESI24 ^{13}C NMR spectrum of prealnumycin (**2**).

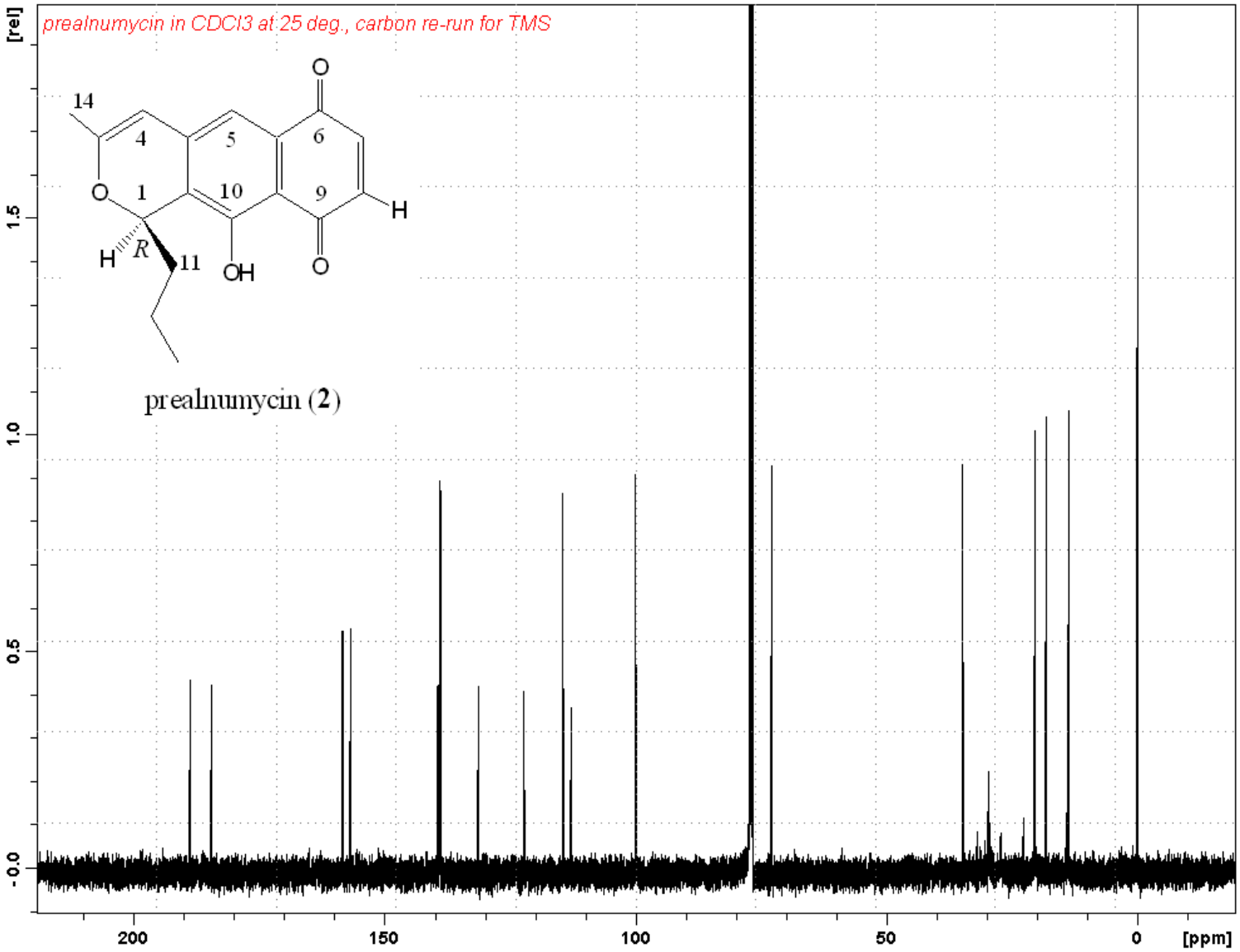

Fig. ESI25 HSQC spectrum of prealnumycin (**2**).

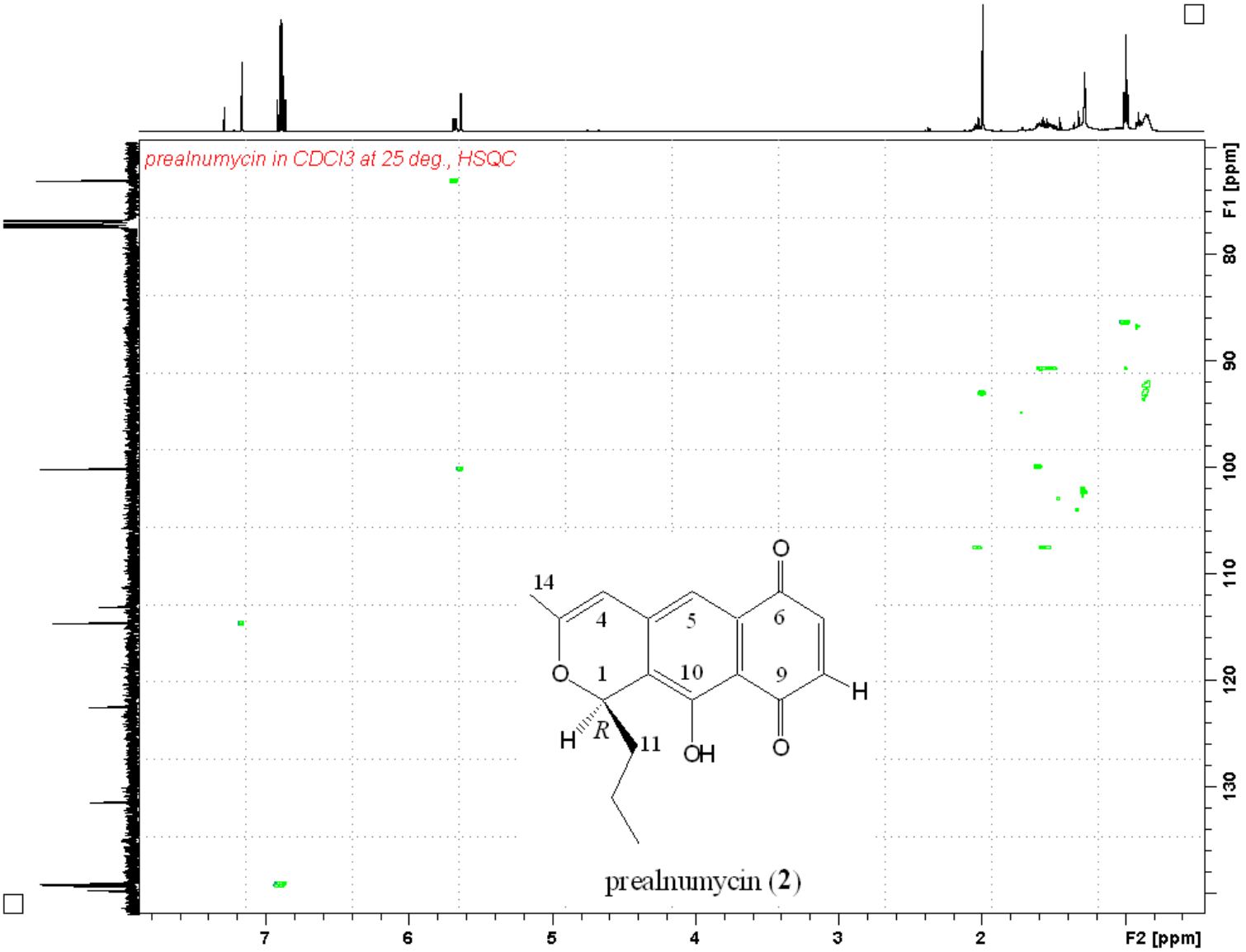

Fig. ESI26 HMBC spectrum of prealnumycin (**2**).